ORIGINAL ARTICLE

Cognition-based MRI brain tumor segmentation technique using modified level set method

Virupakshappa[1] · Basavaraj Amarapur[2]

Abstract

Gliomas are the most common types of brain tumors seen in adults. Generally, it starts from glioma cells and affects the adjacent tissues. Even though the analysis of glioma has well developed, the identification is still poor. In this paper, we propose an efficient modified level set method for brain tumor segmentation, in which we preprocess the image to remove the noise and then accurately segment the magnetic resonance images (MRI). Therefore, this document anticipated an innovative level set algorithm for segmenting gliomas from the MRI brain images where the segmentation is made automatically by means of selecting the initial contour automatically from the maximum intensity pixel computed from the histogram intensity plots. The proposed methodology is implemented in the working platform of MATLAB to produce 99% accuracy, and the results are analyzed by the existing methods.

Keywords Magnetic resonance images · Median filter · Histogram equalization · Modified level set segmentation · Perona–Malik diffusion (PMD) filter

1 Introduction

Brain tumor is a type of cancer, which is the second leading cause of death among children, adults and elder people (Dubey et al. 2011; Sandager et al. 2015). The abnormal growth of cells generates a cluster inside the brain which is recognized as brain tumor. In the condition of brain tumor, the tissue identification is made by using magnetic resonance imaging because it offers many advantages for noninvasive imaging techniques (Farhi et al. 2017).

The tumor growth may be faster or slower which is based on the type and condition of the patient health. The tumors that originate in the brain are called primary tumors (like glioblastoma multiforme, meningioma, astrocytoma, etc.). The tumors that originate in other parts of the body and spread to the brain are known as secondary tumors (Haritha 2016).

✉ Virupakshappa
  virupakshi.108@gmail.com

  Basavaraj Amarapur
  bamarapur@yahoo.com

1 Department of C S E, Appa Institute of Engineering &
   Technology, Kalaburagi, Karnataka, India

2 Department of E & E, Poojya Doddappa Appa College
   of Engineering, Kalaburagi, Karnataka, India

A primary or secondary tumor is based on the basis. The brain tumors normally affect cerebrospinal fluid (CSF), which leads to strokes (Jose et al. 2014). The structure of the brain is generally scanned by various imaging modalities including computed tomography (Abdel-Maksoud et al. 2015) and MRI imaging.

Imaging techniques allow medical practitioners and researchers to evaluate activities and disorders in the human brain, before invasive surgery is performed. Among several medical imaging modalities, magnetic resonance imaging provides more preferred contrast information about brain tissues (Jui et al. 2015).

The brain MR image data are creating an innovative possibility for neurosurgeons and medical scientists. Therefore, the analysis and processing of the image data are used to develop the analytical competence of physicians (Zhang et al. 2017) and reduce the required time for exact analysis, which is executed by computer-aided diagnosis (CAD) system for patient treatment and monitoring (Doupi et al. 2015; Jepsen et al. 2015).

In image processing, segmentation of brain tumor is referred as the technique of isolating tumor image into mutually exclusive regions. It is applied to identify objects of interest and edges or boundaries of images (Vishnumurthy et al. 2016).

Brain tumor and its segmentation are still a wide research area. Since it plays important role in the MRI processing and computer vision, it is considered as a significant step for several medical applications (Beddad and Hachemi 2016).

Various clustering techniques are used to segment the images. Hard-type clustering techniques indicate an object that can belong to only one cluster, resulting in very definitive segmentation. Here, the level set segmentation method is derived from the standard partial differential equations. It works by continuously calculating the differences between pixels. Here, the images are segmented easily by well-defined mathematical techniques and methods. Another common type of segmentation technique is the watershed segmentation technique which is a region-based segmentation technique, and it continuously searches the pixels and regions (Kapoor and Thakur 2017).

Cellular automata (CA) is another segmentation method, which is effectively executed in several advanced studies. Here, CA-related segmentation algorithm is used to tackle the global optimization with diverse datasets which are robust against noise (Sompong and Wongthanavasu 2017).

This innovative technique involves the process of MR image segmentation using modified level set segmentation method. A brief introduction about the brain tumor, its types, segmentation and computer-aided diagnosis is given in Sect. 1, and the research works related to our proposed method are given in Sect. 2. Moreover, Sect. 3 includes the background information of existing level set method. Also, a detailed description of our proposed method using modified level set segmentation method is given in Sect. 4. The test outcomes and relative analysis are presented in Sect. 5. In the end, conclusions are drawn in Sect. 6.

2 Related works

Latif et al. (2017) anticipated a classification and segmentation procedure for low-grade and high-grade glioma tumors in multimodal magnetic resonance (MR) images. In the system, each multimodal MR image is divided into small blocks and features. These attributes are extracted by 3-dimensional discrete wavelet transform (3D DWT). Random forest classifier is used for the classification of multiple glioma tumor classes, and then, segmentation is performed by reconstructing the MR image which is based on the classified blocks. MICCAI BRATS dataset is used to examine the technique, and experiments are performed for low-grade glioma (LGG) and high-grade glioma (HGG) datasets. These results are compared by dissimilar classifiers like multilayer perception, radial basis task, naive Bayes. After this analysis, random forest classifier is providing a better precision by securing average accuracy of 89.75 and 86.87% which is obtained for HGG and LGG, respectively.

Mohan and Subashini (2018) proposed the segmentation and tumor grade classification techniques for brain magnetic resonance (MR) images. In magnetic resonance imaging, the tumor may be understandable, but physicians require quantification for additional treatment. Here, the hybrid procedures supply a second estimation and support for radiologists to accept medical images which are used to develop the analytical exactness. This article is used to review the existing trends in segmentation and classification which are appropriate for tumor-infected human brain MR images through a target on gliomas and astrocytoma.

Kanas et al. (2015) analyzed various MR imaging modalities for detecting and segmenting the brain images consisting of neoplasms. They have considered the following types: T1 weighted, T2 weighted, gadolinium-enhanced T1 weighted and FLAIR types. Here, segmentation was carried out using various methods including outlier detection and clustering healthy tissues. The framework was implemented using the dataset consisting of 57 patient's images and 25 synthetic images. Performance evaluation was carried out using Dice coefficient and sensitivity analysis.

Pereira et al. (2016) proposed a segmentation technique which relies on convolutional neural networks (CNNs) using small kernels of size 3 × 3. The small kernel is used to design a deeper architecture having a positive effect on overfitting which is specified by the fewer quantity of weight in the network. They have used intensity normalization method for preprocessing the image.

Ramakrishnan and Sankaragomathi (2017) had examined the classification of CT images into tumor or non-tumor images; then, segmentation of tumor is carried out. The classification of images was performed using support vector machine (SVM), and segmentation was performed using modified region growing (MRG) technique along with threshold optimization. Many algorithms like evolutionary programming, gray wolf optimization (GWO), harmony search are exploited. The experimental results proved better accuracy of 99.05% for MRG-GWO.

Vishnuvarthanan et al. (2017) analyzed the larger volumes of patient data by using automated algorithm. The algorithm was used to identify the tumor region surrounded by normal tissue portions and edema regions. The proposed method involves optimization techniques as well as clustering methods. Bacteria foraging optimization is used for optimization, and segmentation is carried out using modified fuzzy C means. Various parameters were used for performance evaluation of the proposed method.

Liu et al. (2014) presented a survey of segmentation methods for brain tumors in MR images. They gave small introduction about tumors, its types and various imaging technologies followed by various preprocessing methods. Finally, they discussed about segmentation techniques. They

have also discussed about evaluation methods and validation of the obtained results of segmentation.

Gui et al. (2017) proposed a segmentation method motivated by the isoperimetric inequality in differential geometry, in which the isoperimetric constraint was integrated into a level set framework to penalize the ratio of its squared perimeter to its enclosed area of an active contour. This model can ensure the compactness of segmenting objects and complete missing and/or blurred parts of their boundaries simultaneously. The isoperimetric shape constraint was free of explicit expressions of shapes, and it is scale-invariant. As a result, the method could handle various objects with different scales and did not need to estimate parameters of shapes. The method can also segment lesions with blurred and/or partially missing boundaries in ultrasound, computed tomography (CT) and magnetic resonance images efficiently.

Yang et al. (2017) proposed a hierarchical level set clustering approach to segment prostate from MR image, which makes full use of statistics information of manual segmentation result and incorporates shape prior into the segmentation task. The medium slice of prostate MR data, which was segmented artificially, was used to offer prior information and guide the segmentation of other slices. The Bhattacharyya coefficient between manual segmentation result of medium slice and local block region of pending slice was calculated to estimate the likelihood of local prostate region in pending slice. An adaptive blurring process was implemented before the optimization of level set function to restrain the redundancy texture information and retain the edge information in the meantime. The method captures the contour of prostate with a level set evolution embedded shape prior which was derived from the segmented result of medium slice.

Suresh et al. (2017) proposed an efficient modified level set method for brain tumor segmentation, in which they preprocess the image to remove the noise and then accurately segment the MR images.

3 Background of level set segmentation

The level set methods are used to identify the image limitations. The fundamental scheme of the level set process is represented by the zero level set for an advanced dimensional task, which is recognized as a level set method (Anam et al. 2014; Suresh 2014). The movement of the structure is created by means of the progression of the level set task.

Let us consider a dynamic parametric line as $O(p(f, d), q(f, d))$. The curve development is specified as

$$\frac{\partial O}{\partial d} = s_f V \tag{1}$$

where d is the set point; V is the innermost vector to the curve O; s_f is the speed task which is used to maintain the movement of the line; and f is the curve limitation.

The development of level set is derived from the above Eq. (1) which is used to implanting the dynamic line as the zero level set and a time-dependent level set task $L(p, q, d)$. Moreover, the embedding level set task obtains the negative values as the inside zero level line and the positive values as the outside zero level line.

So, the inward vector to the curve O is specified as

$$V = -\frac{\nabla L}{|\nabla L|} \tag{2}$$

Here, ∇ is the gradient operator. The level set evolution equation obtained from curve evolution is given as:

$$\frac{\partial L}{\partial d} = s_f |\nabla L| \tag{3}$$

The above equation is equivalent to

$$\begin{aligned} \frac{\partial L}{\partial d} &= \chi \times div(x_n(|\nabla L|)|\nabla L|) \\ &+ \delta G_E(L) div\left(g \frac{\nabla L}{(|\nabla L|)(|\nabla L|)}\right) + \beta s_f G_E(L) \end{aligned} \tag{4}$$

where G_E is the direct delta function; $div()$ is the divergence operator; and s_f is the speed function. Also, β, δ and χ are the coefficients of level set equation, which are user-defined parameters.

Moreover, the speed function is given as

$$s_f = \frac{1}{\left(1 + \left|\nabla\left(M_F \times B\right)\right|\right)} \tag{5}$$

where M_F is the Gaussian filter and B is the image.

However, the level set method is efficient, but it requires manual initialization to proceed the level set task. Hence, we have modified the level set method for the automatic initialization of initial contours and to improve the segmentation accuracy.

4 Proposed brain tumor segmentation method using modified level set segmentation algorithm

A glioma is a significant kind of tumor which starts from glial cells in the brain or spine. Normally, gliomas are classified by their position which is determined by pathologic assessment of the tumor. Here, low-grade gliomas are well discriminated (not anaplastic). It is used to express gentle tendency and an enhanced prediction for the patient. On the other hand, it is categorized as malignant because they encompass a consistent rate of repetition and position.

**Fig. 1** Block diagram of proposed brain tumor segmentation method
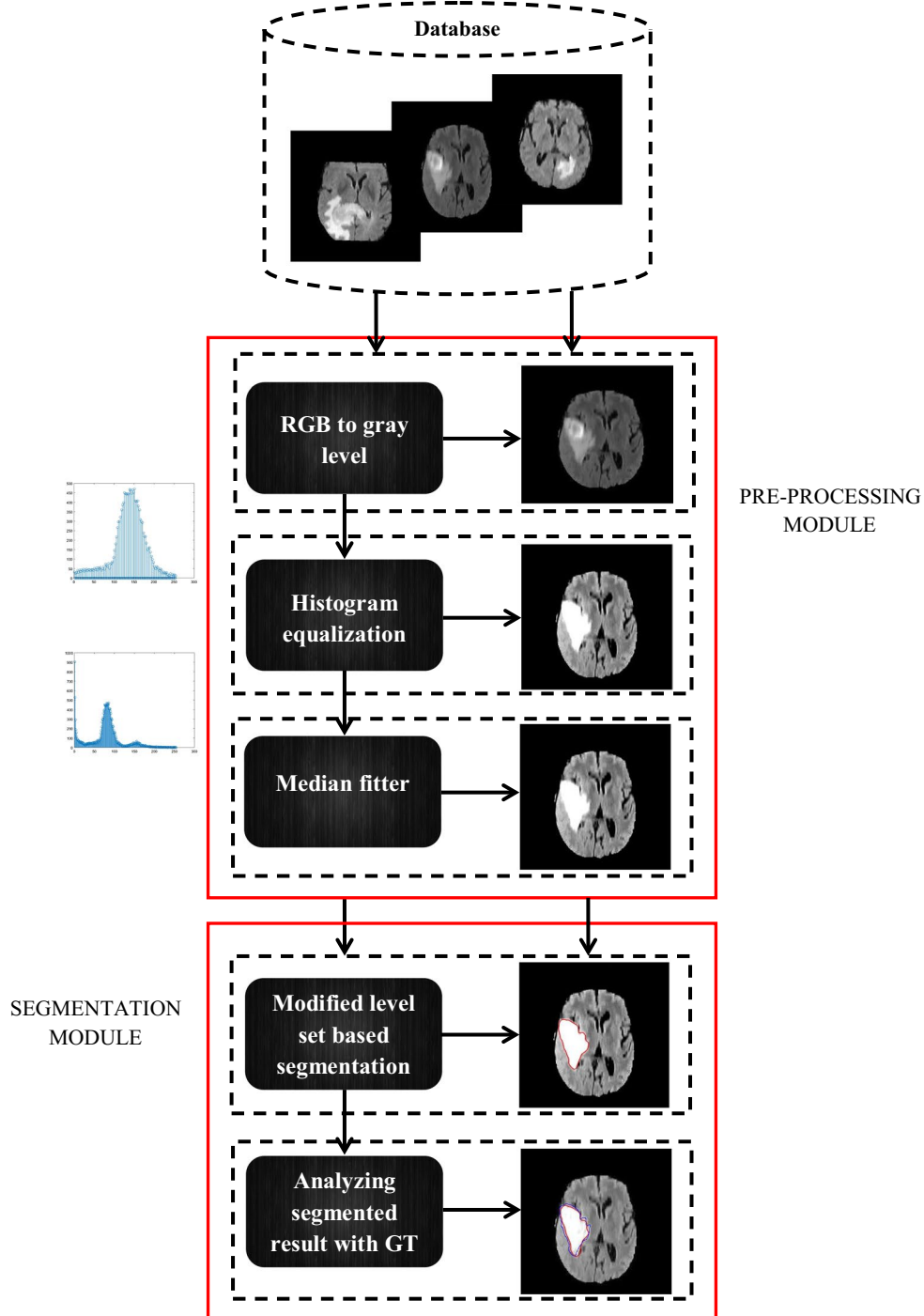
High-grade gliomas are undifferentiated or anaplastic. It is hateful and carries a bad prediction. High-grade gliomas (HGGs) generally contain glioblastoma (GBM) and anaplastic astrocytoma (AA), which are the common brain tumors in adults.

The high-grade gliomas contain a medium survival rate, so they require immediate treatment. The slow-growing low-grade variants like low-grade astrocytomas or oligodendrogliomas take several years to grow, so aggressive treatment can be postponed as long as possible.

MRI is a significant tool for surgeons. The advantage of MR imaging techniques is the capability to model not only the complete lesion, but also the nearby brain tissue for physiologic and metabolite alterations in cerebral gliomas.

Hence, this document illustrates about an effective modified level set segmentation method for segmenting the
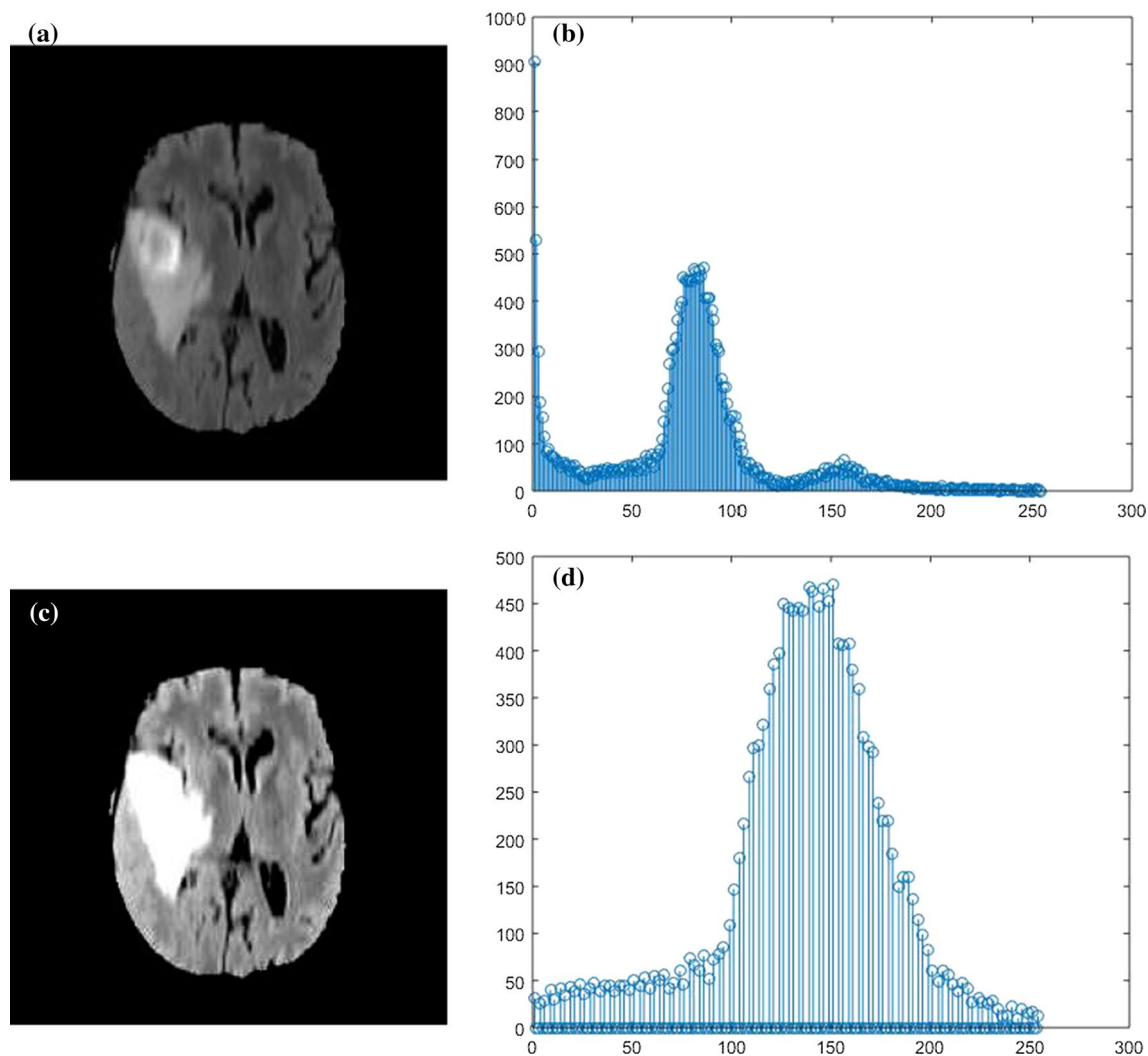
Fig. 2 **a** Original gray image; **b** histogram plot; **c** histogram equalized image; **d** histogram plot for contrast-enhanced image

gliomas from the brain MRIs. The proposed technique is composed of two modules.

- Preprocessing module.
- Segmentation module.

The block diagram of proposed brain tumor segmentation method is given in Fig. 1.

In the preprocessing module, the RGB to gray level conversion, histogram equalization and median filtering steps are done in order to remove the unwanted noise contents, whereas in segmentation module, the proposed modified level set segmentation method is employed for the segmentation of tumor part from the brain MRIs. Finally, the segmentation efficiency of the proposed approach is analyzed using their ground truth (GT) samples.

Further, the steps involved in the proposed model are detailed in the upcoming sections.

4.1 Preprocessing module

Preprocessing is the fundamental step of image processing technique. In general, the medical images should be preprocessed to reduce the unwanted noise components as well as the computation complexity. Here, color-to-gray conversion is performed to reduce the processing complexity. Along with this, the preprocessing process is carried out using histogram equalization (HE) method and the median filtering technique to remove the unwanted noise.

4.1.1 Median filter

Median filter is used to replace the middle pixel by way of gray levels in a window which slides each pixel in the image. Here, the filter $(b \times b | b = 3, 5, \ldots)$ is considered as square windows of odd size. It is the general structure of median filter. For a given $(M \times N)$ image, $\text{Im} g(p, q)$ with

$(p, q) \in \{1, 2, \ldots, M\} \times \{1, 2, \ldots, N\}$, a 2-dimensional $(b \times b)$ median filter can be defined as:

$$MF(\text{Im } g(k, l)) = \text{median}\{\text{Im } g(p + s, q + t)\} \qquad (6)$$

where $s, t \in \left(-\left(\frac{b-1}{2}\right), \ldots, \left(\frac{b-1}{2}\right)\right)$ and $\text{Im } g(p, q)$ is the pixel value at point (p, q).

A notable property of the median filter is equipped for smoothing an image while preserving its edges. Therefore, the median filter is frequently used as a de-noising filter.

4.1.2 Histogram equalization

In this step, the image contrast is enhanced with the help of histogram equalization technique. Histogram equalization operation is widening the intensity values with the total range of values which is used to carry out the high contrast. Suppose, if the image is represented by close contrast values like the background and foreground being bright or dark at the same time, then this method is helpful.

Histogram equalization is a mapping of gray levels 'u' as gray levels 'x.' Here, the sharing of gray level 'x' is identical. The mapping is used to stretch the contrast for gray levels through expanding the range of gray levels in the histogram maxima. Since the contrast is expanded in image pixels, the transformation develops the delectability of image features.

The probability density function of a pixel intensity level 'a_v' is specified as:

$$\text{PDF}_a(a_v) = \frac{b_v}{b} \qquad (7)$$

where $0 \leqslant a_v \leqslant 1$, $v = 0, 1, \ldots, 255$; b_v is the number of pixels at intensity level 'a_v,' and b denotes the total number of pixels.

Now, the histogram can be derived by plotting $\text{PDF}_a(a_v)$ against a_v. At this time, a new intensity level d_v is produced as defined as

$$d_v = \sum_{z=0}^{v} \frac{b_z}{b} = \sum_{z=0}^{v} \text{PDF}_a(a_z) \qquad (8)$$

Here, the results are used to modify the intensity of each pixel through its local neighborhood. Suppose, if the image encompasses a great dissimilarity among the highest and lowest intensity levels, then the image has high contrast. Therefore, the region of lower contrast obtains a higher contrast devoid of affecting the global contrast through equalizing the histogram of image.

Figure 2 shows the histogram plots for the median filtered image and the histogram equalized image.

Figure 2c shows the histogram plot after equalization, which is clearer than the median filtered image. After

enhancing the image contrast, the images are subjected to segmentation process.

4.2 Segmentation module

The main goal of the segmentation is to isolate the region of interest from its background. After preprocessing, image is segmented by modified level set segmentation method.

In this segmentation module, the preprocessed brain MRIs obtained from the patients with the glioma, which is to be classified as high-grade gliomas and low-grade gliomas, are segmented by modified level set segmentation method.

The level set method is a robust, precise, and competent procedure which is mainly used for a broad group of problems. Also, the conventional level set segmentation method contains certain drawbacks such as they require considerable information like proper velocity (i.e., it requires manual initialization) to proceed the level set task, so modification to the level set is must in order to increase segmentation accuracy.

4.2.1 Modified automated level set segmentation method

The issues from conventional level set segmentation algorithm are overcome by the proposed modified level set segmentation. The proposed algorithm provides automatic initialization for finding the initial contour as the maximum pixel point which is obtained from the image histogram, and it enables automatic segmentation for any kind of images.

Moreover, the proposed level set segmentation method utilizes the anisotropic diffusion filter instead of Gaussian filter. It is proposed by Perona and Malik. The PMD filter has few advantages than Gaussian filter, because employing Gaussian filter takes more time and reduces details of images. In PMD filter, the object boundaries are used to smoothen the noise and make the regions distinct. Moreover, the local edges are enhanced by discontinuities like boundaries. So, the noise is competently removed and object contours are strongly enhanced.

The PMD filter smoothens the image with the help of a diffusion parameter which is interpreted as an image convolution by a Gaussian kernel. It is specified as follows

$$B(p, q, d) = B_0(p, q) \times M_F(p, q, d) \qquad (9)$$

Also, the anisotropic diffusion equation is given as

$$B_d = \frac{\partial B}{\partial d} = e_s(\|\nabla B(p, q, d)\|)\Delta B + \nabla\left[e_s(\|\nabla B(p, q, d)\|)\right]\nabla B \qquad (10)$$

In the above equation, the term $e_s(\|\nabla B(p, q, d)\|)$ is the diffusion coefficient, ∇B is a gradient image, and $e_s()$ is an edge termination task.
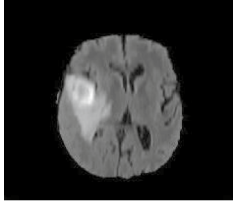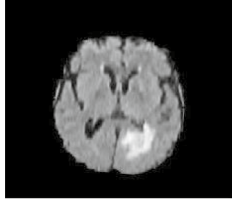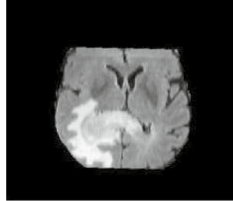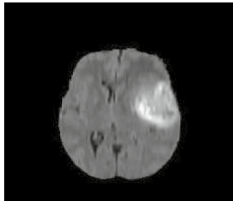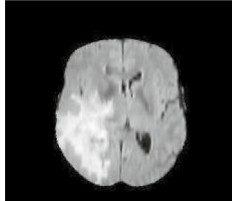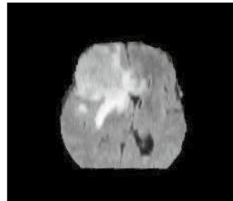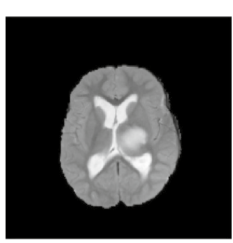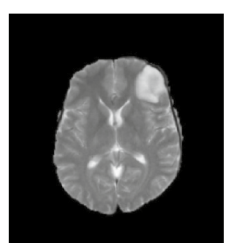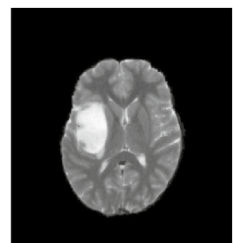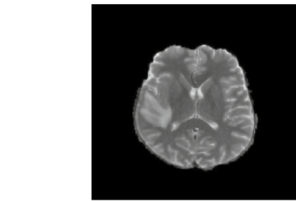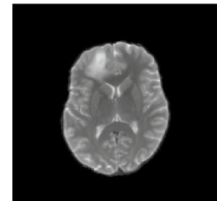
IMAGE TYPE	IMAGES		
High Grade Glioma (HGG)	HG_1	HG_2	HG_3
	HG_4	HG_5	HG_6
Low Grade Glioma (LGG)	LG_1	LG_2	LG_3
	LG_4	LG_5	

Fig. 3 Input database images

4.2.2 Steps involved in modified automated level set segmentation method

In the modified automated level set segmentation method, the involved steps are given as follows

Step 1: Find image entropy
Initially, the image entropy is used to find the information about the image. Moreover, the entropy measures the loss of image information and it is expressed as follows.

$$\text{Ent}(u, v) = - \sum_{z=0}^{255} g(z)\log_2(g(z)) \tag{11}$$

Step 2: Apply PMD filter
Here, the Perona–Malik diffusion (PMD) (Vishnuvarthanan et al. 2017) filter is used to smoothen the images instead of Gaussian filter.

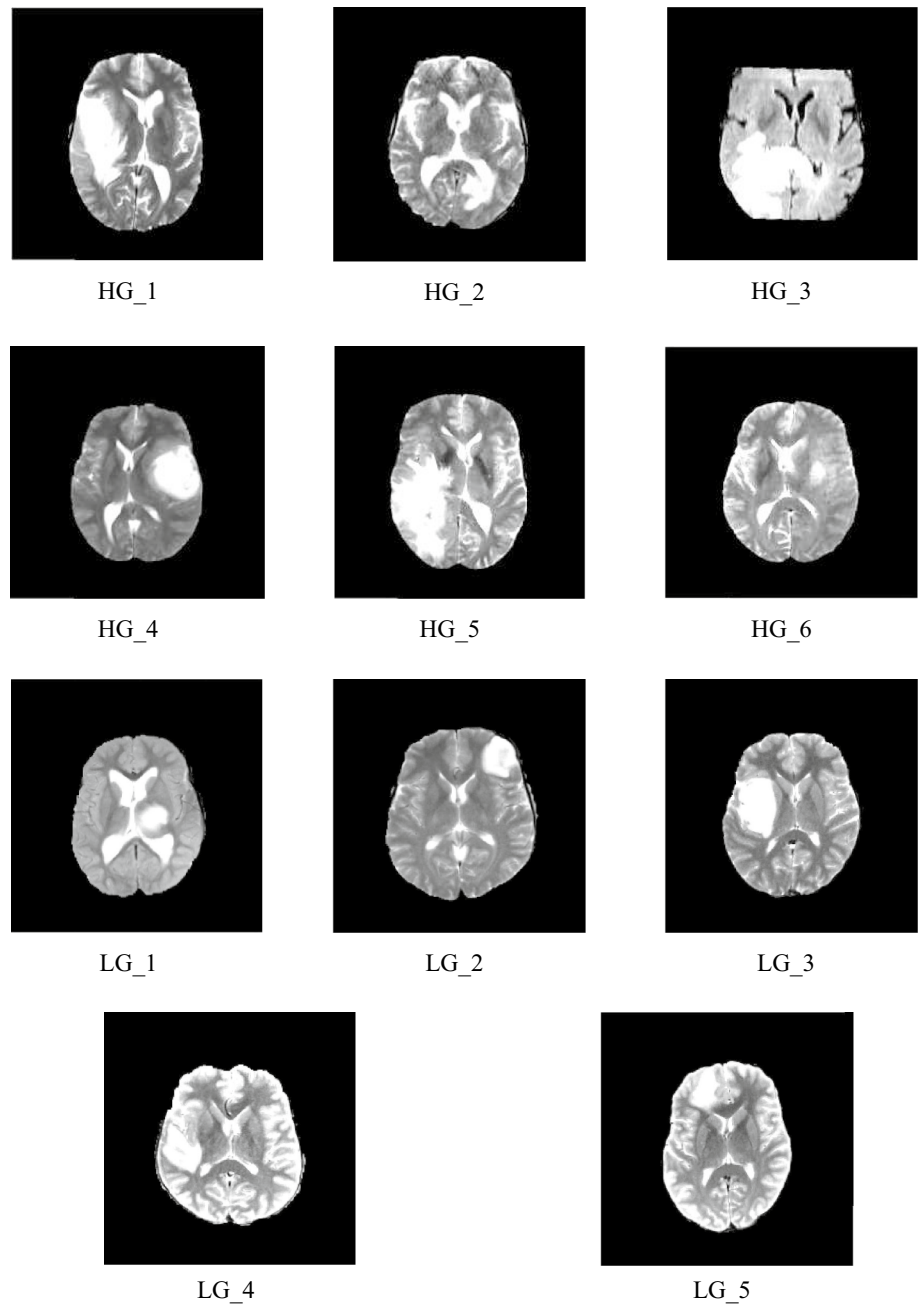#### Step 3: Calculate image gradient magnitude
In this step, the image gradient magnitude is obtained as

$$M_{\text{norm}} = \frac{|\nabla B(p, q)| - \min(|\nabla B(p, q)|)}{\max|\nabla B(p, q)| - \min|\nabla B(p, q)|} \tag{12}$$

Step 4: Estimate modified speed function
Now, the modified speed function is calculated in the below equation

Fig. 4 Preprocessed brain MR
images

HG_1   HG_2   HG_3

HG_4   HG_5   HG_6

LG_1   LG_2   LG_3

LG_4   LG_5

$$\hat{s}_f = \exp\left(-cM_{\text{norm}}^2\right) \tag{13}$$

In the above equation, c is a parameter for controlling the
motion of contour.

Step 5: Determine initial contour using histogram
Find the histogram Hist $(B(x, y))$ of each pixel locations
in the images. Set the peak intensity pixel as the initial
contour.

Step 6: Discover new contour
The new contour is found by the below contour evolution
equation

$$\frac{\partial L}{\partial d} = \chi \times div(x_n(|\nabla L|)|\nabla L|)$$
$$+ \delta G_E(L)div\left(g\frac{\nabla L}{(|\nabla L|)(|\nabla L|)}\right) + \beta s_f G_E(L) \tag{14}$$
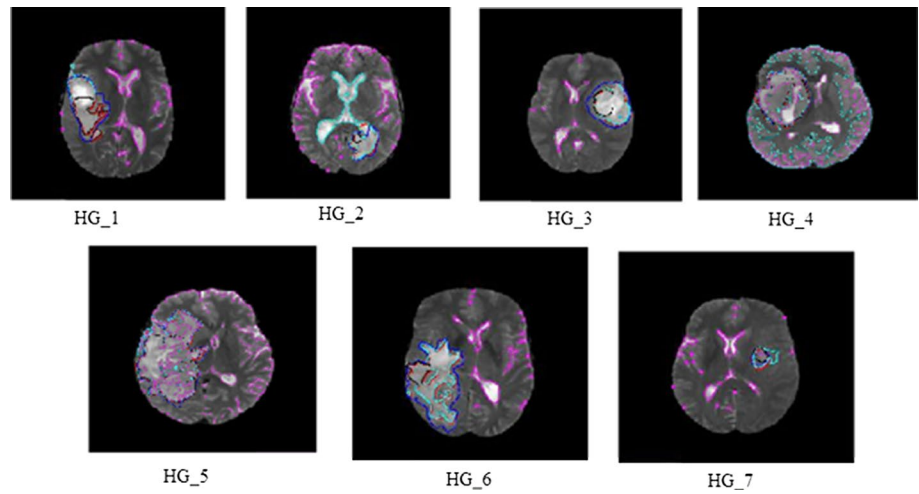
Step 7: Repeat
The finding of new contour is repeated until it congre-
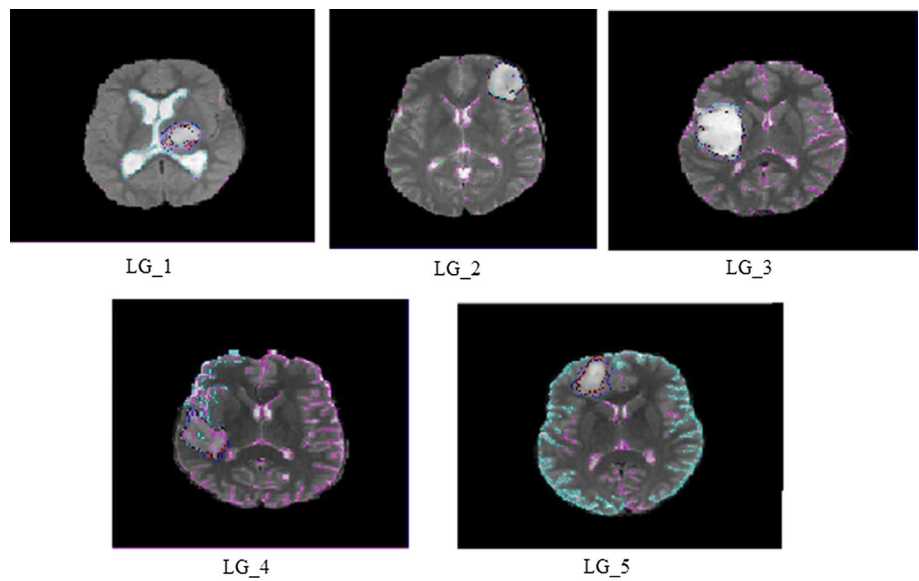gates or the maximum iteration is obtained.
Once the segmentation process is done, the boundary of
tumor portion will be obtained. Further, it can be sepa-
rated from the brain MRIs for analysis of its category.

Fig. 5 HGG brain tumor images (color figure online)

Fig. 6 LGG brain tumor images (color figure online)

Table 1 Sensitivity, specificity and accuracy values for the segmentation result of the proposed modified level set method

Image type	Image name	Sensitivity	Specificity	Accuracy
HGG	HG_1	0.952381	0.993424	0.991826
	HG_2	0.794212	0.9979	0.994516
	HG_3	0.705496	1	0.988742
LGG	LG_1	0.72412	0.998576	0.996069
	LG_2	0.939107	0.999479	0.998447
	LG_3	0.849996	0.998129	0.993596

Table 2 Sensitivity, specificity and accuracy values for the segmentation result of existing region growing method

Image type	Image name	Sensitivity	Specificity	Accuracy
HGG	HG_1	0.892063	0.994526	0.990537
	HG_2	0.737406	0.974491	0.970553
	HG_3	0.660404	1	0.987019
LGG	LG_1	0.710457	0.967343	0.964996
	LG_2	0.838231	0.999823	0.997061
	LG_3	0.83745	0.998271	0.993349

5 Result and discussion

In this section, the result and discussion is illustrated about the modified level set process with MRI brain tumor segmentation. The proposed algorithm is executed in the MATLAB platform. The experimentation is carried out in a system which contains 4 GB RAM and 2.10 GHz Intel i-3 processor.

Table 3 Sensitivity, specificity and accuracy values for the segmentation result of the existing FCM method

Image type	Image name	Sensitivity	Specificity	Accuracy
HGG	HG_1	0.885261	0.96429	0.961214
	HG_2	0.729904	0.950521	0.946856
	HG_3	0.68295	0.988948	0.977251
LGG	LG_1	0.746978	0.964596	0.962608
	LG_2	0.859424	0.986313	0.984144
	LG_3	0.839186	0.983563	0.979145

Table 4 Sensitivity, specificity and accuracy values for the segmentation result of the existing K means method

Image type	Image name	Sensitivity	Specificity	Accuracy
HGG	HG_1	0.885261	0.96429	0.961214
	HG_2	0.742765	0.948692	0.945271
	HG_3	0.660404	0.989546	0.976964
LGG	LG_1	0.746978	0.964596	0.962608
	LG_2	0.846426	0.98702	0.984617
	LG_3	0.841079	0.982896	0.978555

Table 5 Sensitivity, specificity and accuracy values for the segmentation result of the existing level set method

Image type	Image name	Sensitivity	Specificity	Accuracy
HGG	HG_1	0.553288	0.980139	0.553288
	HG_2	0.999964	0.98492	0.094319
	HG_3	1	0.972655	0.284641
LGG	LG_1	0.473726	0.999649	0.994845
	LG_2	0.893473	0.999764	0.997947
	LG_3	0.745917	0.999539	0.991777

Table 6 Jaccard, Dice and Hausdorff distance values for the segmentation result of the proposed modified level set method

Image type	Image name	Jaccard	Dice	Hausdorff
HGG	HG_1	0.625767	0.006171	0.008114
	HG_2	0.365767	0.006365	0.009098
	HG_3	0.479566	0.005594	0.010098
LGG	LG_1	0.274774	0.004513	0.001646
	LG_2	0.442046	0.004547	0.007129
	LG_3	0.486081	0.00407	0.007274

Table 7 Jaccard, Dice and Hausdorff distance values for the segmentation result of the existing region-based growing method

Image type	Image name	Jaccard	Dice	Hausdorff
HGG	HG_1	0.5682	0.005752	8.38E−03
	HG_2	0.218468	0.003165	0.019364
	HG_3	0.448914	0.00536	0.00985
LGG	LG_1	0.145923	0.001705	0.005007
	LG_2	0.380798	0.004097	0.007181
	LG_3	0.472513	0.003981	0.007274

Table 8 Jaccard, Dice and Hausdorff distance values for the segmentation result of the existing FCM method

Image type	Image name	Jaccard	Dice	Hausdorff
HGG	HG_1	0.392197	0.0044	0.014134
	HG_2	0.157949	0.002172	0.023457
	HG_3	0.39044	0.004584	0.015562
LGG	LG_1	0.150635	0.001724	0.01458
	LG_2	0.289988	0.003088	0.007143
	LG_3	0.378235	0.003401	0.007183

Table 9 Jaccard, Dice and Hausdorff distance values for the segmentation result of the existing k means method

Image type	Image name	Jaccard	Dice	Hausdorff
HGG	HG_1	0.392197	0.0044	1.41E−02
	HG_2	0.157154	0.00216	0.02358
	HG_3	0.380823	0.004509	1.56E−02
LGG	LG_1	0.150635	0.001724	0.01458
	LG_2	0.289029	0.003083	0.007166
	LG_3	0.376107	0.003391	0.007183

Table 10 Jaccard, Dice and Hausdorff distance values for the segmentation result of the existing level set method

Image type	Image name	Jaccard	Dice	Hausdorff
HGG	HG_1	0.354218	0.00441	1.21E−02
	HG_2	0.040341	0.001339	0.010902
	HG_3	0.193487	0.003154	1.27E−02
LGG	LG_1	0.160066	0.003132	0.002106
	LG_2	0.408332	0.004304	0.007174
	LG_3	0.42133	0.003697	0.007388

For performance analysis of the proposed automated brain tumor segmentation and to compare between different methods, the medical records of the patients with brain tumor problems were collected from the multimodal brain tumor image segmentation benchmark (BRATS) challenge in conjunction with the international conference on medical image computing and computer-assisted interventions (MICCAI 2015). These acquired data were preprocessed, analyzed and classified for abnormality detection in patients.
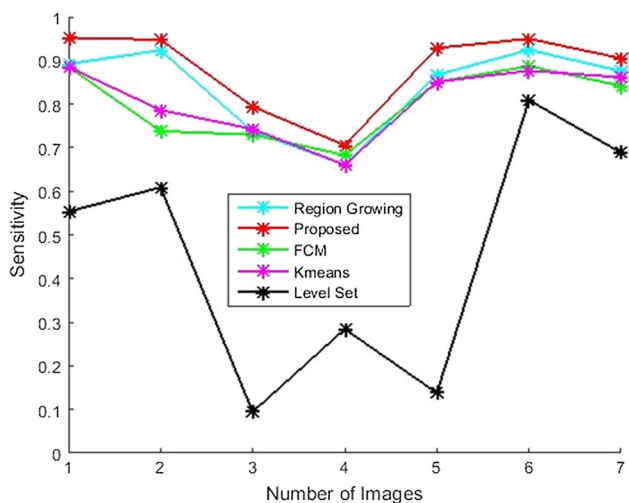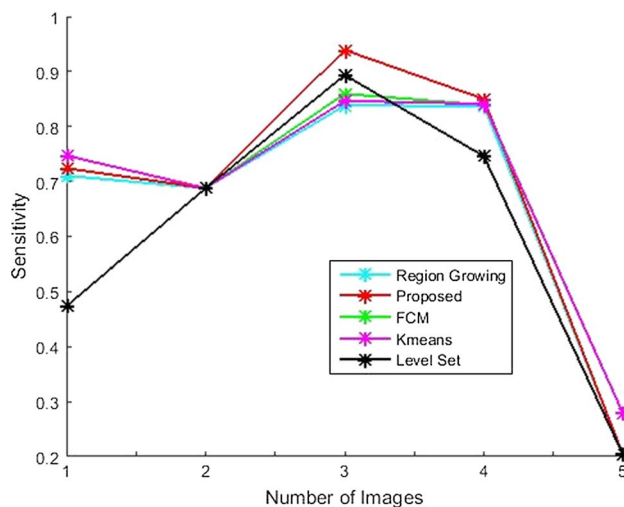
Fig. 7 Sensitivity comparison plot for proposed versus existing techniques (HGG) (color figure online)
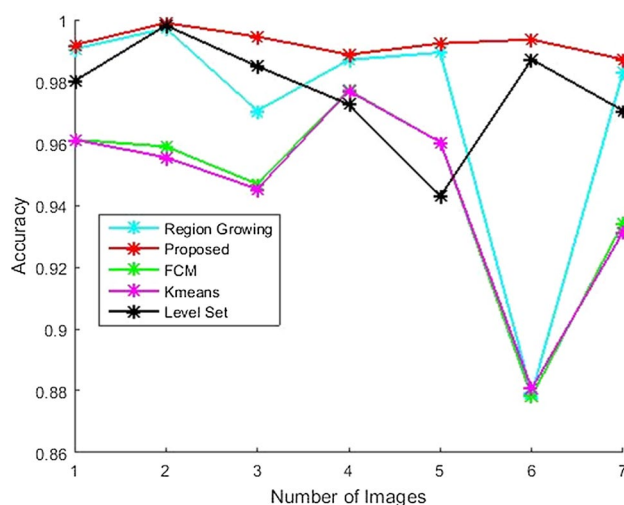
Fig. 9 Accuracy comparison plot for proposed versus existing techniques (HGG) (color figure online)
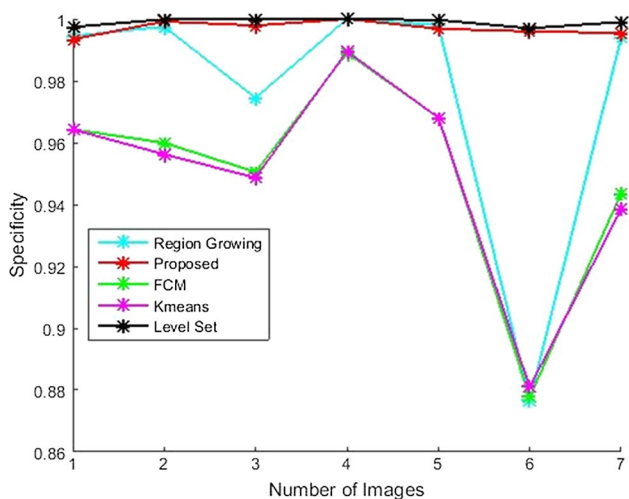
Fig. 8 Specificity comparison plot for proposed versus existing techniques (HGG) (color figure online)

Fig. 10 Sensitivity comparison plot for proposed versus existing techniques (LGG) (color figure online)

In this experiment, the brain tumor image is identified with the help of modified level set method.

The input HGG and LGG brain tumor images in the database are demonstrated in Fig. 3.

Moreover, the preprocessed brain MRIs of both HGG and LGG are given in Fig. 4.

After pre-processing of the images, the segmentation is carried out by the proposed modified level set method along with various existing segmentation procedures like region-based growing, FCM, *K* means and level set methods the obtained results are presented in the below figures. The actual position is indicated by blue color, and the existing region growing, FCM, *K* means, level set and the proposed modified level set methods are indicated by

sky blue, green, pink, black and red colors, respectively, in Figs. 5 and 6.

The segmented brain tumor images for high-grade glioma (HGG) in the original brain MRI are illustrated in Fig. 5.

The segmented brain tumor image for low-grade glioma (LGG) is illustrated in Fig. 6. All the techniques equally progress on the defected portion of the brain tumor images.

5.1 Performance analysis

This section illustrates about the performance assessment of the proposed modified level set method with brain tumor segmentation. The sensitivity, specificity and accuracy
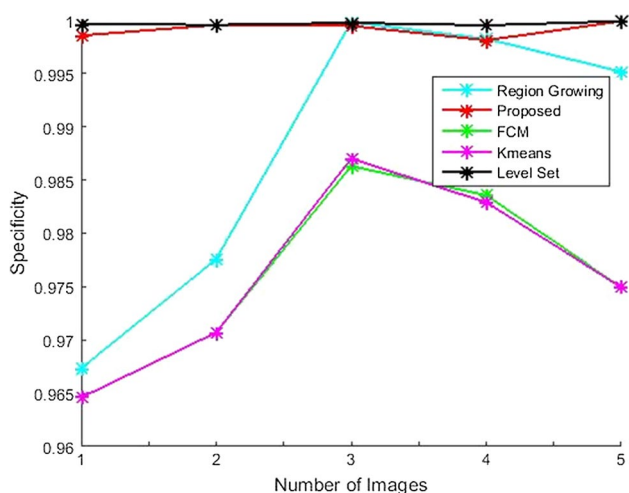
Fig. 11 Specificity comparison plot for proposed versus existing techniques (LGG) (color figure online)
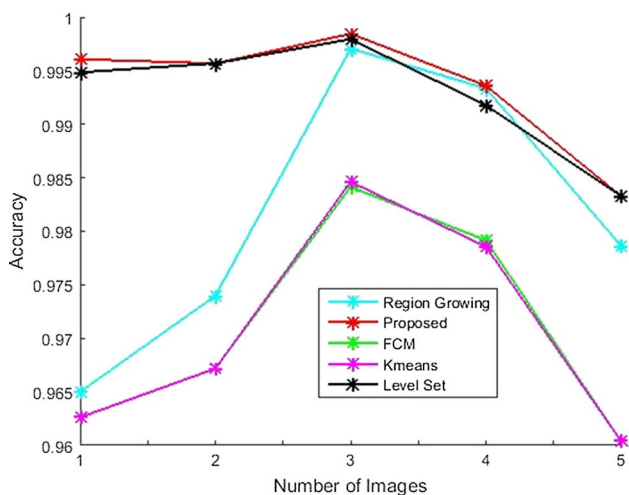
Fig. 12 Accuracy comparison plot for proposed versus existing techniques (LGG) (color figure online)

values computed for the proposed and existing methods are given in Tables 1, 2, 3, 4 and 5.

The above-mentioned tables show that the sensitivity value for HGG images is almost 80% and for LGG is 76%. The specificity value for HGG is 99% and for LGG images is 100%. The accuracy value is proving to be 100% for both HGG and LGG image types.

The sensitivity (56%), specificity (75%) and accuracy (89%) values are obtained for the LGG and HGG image types from the existing approaches like region-based growing, FCM, k means and level set method. Therefore, the proposed modified level set method is more reliable than the existing processes.

By analyzing the tables, it is obvious that the anticipated process is more precise than any other existing techniques.

From Table 1 it is clear that the sensitivity, specificity and accuracy values of the proposed method for the input images are more reliable than the existing methods like region growing, FCM, *k* means and level set.

The distance measure for the HGG and LGG images is illustrated. Here, the proposed method shows minimum distance for Jaccard, Dice and Hausdorff measures, and the existing method proves to be high. The analysis from Tables 6, 7, 8, 9 and 10 clearly shows that the proposed modified level set method is the best for all the segmentation results.

Finally, the segmentation results of proposed and existing techniques for the brain tumor images are plotted in Figs. 7, 8, 9, 10, 11 and 12.

From the comparison plots, it is clear that the proposed modified level set method is more reliable than any other existing techniques. When comparing specificity and accuracy values, the proposed method shows 100% than the existing region growing, FCM, *k* means and level set approaches.

6 Conclusion

In this document, we have designed a modified automated level set-based segmentation algorithm for the precise segmentation of gliomas from the brain MRIs. The proposed algorithm is compared with various state-of-the-art approaches to illustrate the effectiveness of the anticipated process. From the results obtained, it is markedly noted that the proposed modified automated level set-based segmentation technique offers good performance (i.e., average accuracy around 99.3%) in the presence of weak boundaries and it is capable of extracting complex shapes without the knowledge of target shape. In future, we have planned to classify the abnormal brain MRIs affected by the gliomas from the normal MRI brain images.

References

Abdel-Maksoud E, Elmogy M, Al-Awadi R (2015) Brain tumor segmentation based on a hybrid clustering technique. Egypt Inform J 16(1):71–81

Anam S et al (2014) Texture analysis and modified level set method for automatic detection of bone boundaries in hand radiographs. Int J Adv Comput Sci Appl 5(10):117

Beddad B, Hachemi K (2016) Brain tumor detection by using a modified FCM and level set algorithms. In: IEEE control engineering & information technology (CEIT)

Doupi P, Svaar H, Bjørn B, Deilkas E, Nylen U, Rutberg H (2015) Use of the global trigger tool in patient safety improvement efforts: nordic experiences. Cogn Technol Work 17:45–54

Dubey RB, Hanmandlu M, Vasikarla S (2011) Evaluation of three methods for MRI brain tumor segmentation. In: 8th international conference on information technology: new generations

Farhi L, Yusuf A, Raza RH (2017) Adaptive stochastic segmentation via energy-convergence for brain tumor in MR images. J Vis Commun Image Represent 46:303–311

Latif G et al (2017) Multiclass brain glioma tumor classification using block-based 3D wavelet features of MR images. In: Electrical and electronic engineering (ICEEE)

Gui L, Li C, Yang X (2017) Medical image segmentation based on level set and isoperimetric constraint. Physica Med Eur J Med Phys 42:162–173

Haritha D (2016) Comparative study on brain tumor detection techniques. In: Signal processing, communication, power and embedded system (SCOPES)

Jepsen RM, Østergaard D, Dieckmann P (2015) Development of instruments for assessment of individuals' and teams' non-technical skills in healthcare: a critical review. Cogn Technol Work 17(1):63–77

Jose A, Ravi S, Sambath M (2014) Brain tumor segmentation using k-means clustering and fuzzy c-means algorithms and its area calculation. Int J Innov Res Comput Commun Eng 2(3):3496–3501

Jui S-L et al (2015) Brain MR image tumor segmentation with 3-dimensional intracranial structure deformation features. IEEE Intell Syst 31(2):66–76

Kanas VG et al (2015) A low cost approach for brain tumor segmentation based on intensity modeling and 3D random walker. Biomed Signal Process Control 22:19–30

Kapoor L, Thakur S (2017) A survey on brain tumor detection using image processing techniques. In: Cloud computing, data science & engineering-confluence, IEEE

Liu J, Li M, Wang J, Wu F, Liu T, Pan Y (2014) A survey of MRI-based brain tumor segmentation methods. Tsinghua Sci Technol 19(6):578–595

Mohan G, Subashini MM (2018) MRI based medical image analysis: survey on brain tumor grade classification. Biomed Signal Process Control 39:139–161

Pereira S, Pinto A, Alves V, Silva CA (2016) Brain tumor segmentation using convolutional neural networks in MRI images. IEEE Trans Med Imaging 35(5):1240–1251

Ramakrishnan T, Sankaragomathi B (2017) A professional estimate on the computed tomography brain tumor images using SVM-SMO for classification and MRG-GWO for segmentation. Pattern Recogn Lett 94:163–171

Sandager M, Sperling C, Jensen H, Vinter MM, Knudsen JL (2015) Danish cancer patients' perspective on health care: results from a national survey. Cogn Technol Work 17(1):35–44

Sompong C, Wongthanavasu S (2017) An efficient brain tumor segmentation based on cellular automata and improved tumor-cut algorithm. Expert Syst Appl 72:231–244

Suresh A (2014) An efficient view classification of echocardiogram using morphological operations. J Theor Appl Inf Technol (JATIT) 67(3):732–735

Suresh A (2017) Heart disease prediction system using ANN, RBF and CBR. Int J Pure Appl Math (IJPAM) 117(21):199–216

Vishnumurthy TD, Mohana HS, Meshram VA (2016) Automatic segmentation of brain MRI images and tumor detection using morphological techniques. In: 2016 international conference on electrical, electronics, communication, computer and optimization techniques (ICEECCOT)

Vishnuvarthanan A, Rajasekaran MP, Govindaraj V, Zhang Y, Thiyagarajan A (2017) An automated hybrid approach using clustering and nature inspired optimization technique for improved tumor and tissue segmentation in magnetic resonance brain images. Appl Soft Comput 57:399–426

Yang X, Zhan S, Xie D, Zhao H, Kurihara T (2017) Hierarchical prostate MRI segmentation via level set clustering with shape prior. Neurocomputing 257:154–163

Zhang J, Cui X, Li J, Wang R (2017) Imbalanced classification of mental workload using a cost-sensitive majority weighted minority oversampling strategy. Cogn Technol Work 19(4):633–653